The Effects of Ligand Exchange and Mobility on the Peroxidase Activity of a Bacterial Cytochrome c upon Unfolding

Jonathan A. R. Worrall,[a] Rutger E. M. Diederix,[a] Miguel Prudêncio,[a] Christian E. Lowe,[a, b] Simone Ciofi-Baffoni,[b] Marcellus Ubbink,[a] and Gerard W. Canters*[a]

The effect on the heme environment upon unfolding Paracoccus versutus *ferricytochrome c-550 and two site-directed variants, K99E and H118Q, has been assessed through a combination of peroxidase activity increase and one-dimensional NMR spectroscopy. At pH 4.5, the data are consistent with a low- to high-spin heme transition, with the K99E mutation resulting in a protein with increased peroxidase activity in the absence of or at low concentrations of denaturant. Furthermore, the mobility of the polypeptide chain at pH 4.5 for the wild-type protein has been monitored in the absence and presence of denaturant through heteronuclear NMR experiments. The results are discussed in terms of local stability differences between bacterial and mitochondrial cytochromes c that are inferred from peroxidase activity assays. At pH 7.0, a mixture of misligated heme states arising from protein-based ligands assigned to lysine and histidine is detected. At low denaturant concentrations, these partially unfolded misligated heme forms inhibit the peroxidase activity. Data from the K99E mutation at pH 7.0 indicate that K99 is not involved in heme misligation, whereas histidine coordination is proven by the data from the H118Q variant.*

Introduction

The spectroscopically rich properties of the covalently bound heme and the high solubility in both the folded and unfolded state make c-type cytochromes (cyts c) an ideal choice for folding/unfolding studies. Much work has focused on the mitochondrial proteins from horse heart (hh) and the two isoforms from yeast. Kinetics,[1] native-state hydrogen-exchange NMR measurements,[2–4] resonance Raman spectroscopy,[5,6] one- and two-dimensional NMR spectroscopy,[7–10] fluorescence spectroscopy,[11] and EPR, optical, and CD spectroscopies[12] are some of the many biophysical methods that have been employed to gain an insight into the folding/unfolding behavior of these metalloproteins. The loss of the sixth axial methionine ligand to the heme is widely considered to be the first step of the unfolding process, which results in deprotonated protein-based ligands, such as histidine, lysine and the N-terminal α-amino group, as well as solvent molecules competing for the vacant heme coordination site.[6–9,13–17]

The folding/unfolding of bacterial cyts c has received less attention than that of their mitochondrial counterparts. The class I cyt c-550 from the Gram-negative bacterium *Paracoccus versutus* has 134 amino acids and is a member of the larger class of bacterial cyts c.[18] The structure in the ferric state has been solved by X-ray diffraction, which indicates the presence of five α helices and two short stretches of antiparallel β strand, wrapped around the six-coordinate heme with M100 and H19 as the axial ligands (J.A.R.W., unpublished results; Figure 1). Although similar in structure to the well-studied hh cyt c, a number of insertions are present that give rise to the increased size, and sequence homology between the two proteins is very low.[19] Furthermore, in variance to the observations of previous folding/unfolding studies with bacterial cyts,[20–23] cyt c-550 contains one potentially misligating histidine residue, located after the C terminal helix (Figure 1). This position contrasts with the sequence positions of the misligating histidine residues found in hh cyt c (Figure 1), which in an unfolded state has H33 as the predominant nonnative ligand to the heme.[24] In an unfolded state, the H33 misligation prevents proper refolding in the middle segment of the polypeptide chain but does not stop the formation of a proposed early intermediate folding species (or late unfolding species) with interacting N- and C-terminal helices.[13]

Differences in the dynamic properties and folding pathways of class I bacterial cyts c are now starting to be identified, with direct evidence for a bacterial cyt c which refolds along parallel folding pathways.[21] Such pathways have not, as yet, been detected in the mitochondrial proteins and may lead to the question of whether the topology of the native protein is an important determinant of the folding/unfolding mechanism.[25] Therefore, studies on bacterial proteins, which are generally

[a] *Dr. J. A. R. Worrall, Dr. R. E. M. Diederix, Dr. M. Prudêncio, C. E. Lowe, Dr. M. Ubbink, Prof. G. W. Canters*
Leiden Institute of Chemistry, Gorlaeus Laboratories
Leiden University
P.O. Box 9502, 2300 RA Leiden (The Netherlands)
Fax: (+31) 71-527-4349
E-mail: canters@chem.leidenuniv.nl

[b] *C. E. Lowe, Dr. S. Ciofi-Baffoni*
CERM, University of Florence
Via Luigi Sacconi 6, 50019 Sesto Fiorentino, Florence (Italy)

Supporting information for this article is available on the WWW under http://www.chembiochem.org or from the author.

 DOI: 10.1002/cbic.200400291

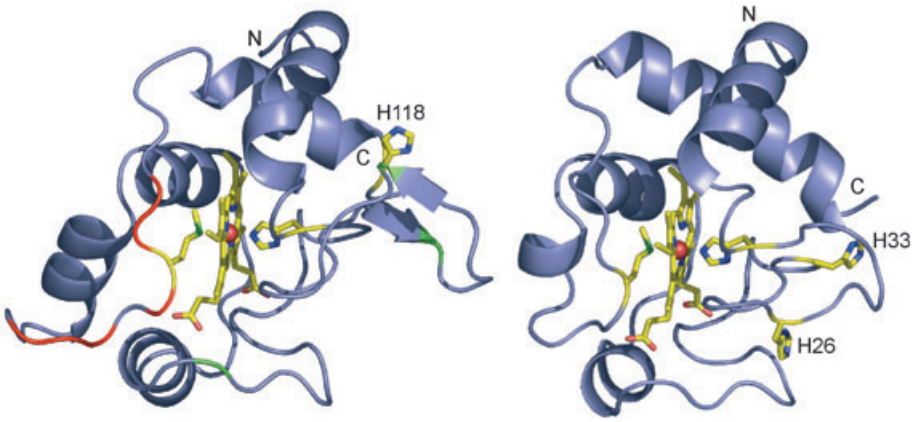

Figure 1. *Comparison of the X-ray crystal structures of* Paracoccus versutus *ferricyt c-550 (left; PDB code: 2BGV, J.A.R.W., unpublished results) and hh ferricyt c (right; PDB code: 1hrc),*[67] *created by using the PyMOL program (available from http://www.pymol.org). The heme and axial ligands are shown as ball-and-stick representations, along with the two histidine residues in hh ferricyt c that are involved in misligation to the heme on the folding/unfolding pathway. H118 in P. versutus ferricyt c-550 is also shown. N and C indicate the N- and C-terminal helices. The colors green (residue numbers 23, 30, and 55) and red (residue numbers 95–97, 99, 101, and 102) on the structure of cyt c-550 highlight regions relating to the* ^{15}N *dynamic data discussed in the text.*

more varied in size and have lower sequence homology between the different species, are important to complement the many studies performed with the mitochondrial proteins.

Previously we have concentrated on the equilibrium unfolding of both mitochondrial and bacterial ferricyts c by monitoring the increase in their peroxidase activity in the presence of denaturant.[26,27] This novel unfolding probe allows information on the lowest free energy unfolding species to be obtained.[26] Clear differences in the total increase in peroxidase activity and the thermodynamic unfolding parameters relating to the lowest free energy unfolding species between the different cyts exist, with the mitochondrial proteins having a less stable methionine ligand interaction in the presence of denaturant.[26]

In the present study the effect of unfolding on the heme environment of cyt c-550 has been assessed at two pH values by using a combination of peroxidase activity assays and 1D NMR spectroscopy. Interpretation of the data for the wild-type (wt) protein has been aided by studying various forms of cyt c-550. We show that despite the unusual sequence position of H118, as compared to the corresponding histidine residue in hh cyt c, this residue and one or more lysine residues (but not K99, which is homologous to K79 in hh cyt c) are involved in ligand-exchange events as the protein unfolds. The effect of these nonnative ligands on the peroxidase activity is assessed. Also, the effect of unfolding at pH 4.5 on the polypeptide chain is monitored through a ^{15}N NMR mobility study.

Results and Discussion

Choice of cyt c-550 variants

At neutral pH values in the presence of denaturant mitochondrial hh cyt c undergoes ligand-exchange events in which lysine or histidine residues can act as nonnative ligands to the heme.[6–8,13] As cyt c-550 contains a single potentially misligating histidine residue,[19] the H118Q variant was constructed to unequivocally test whether histidine ligation is occurring as the protein unfolds. For lysine coordination, K79 and K73 of hh cyt c have been postulated as the nonnative coordinating residues.[8] The lysine residue prior to the axial methionine ligand (K79 in the hh numbering) is conserved in a high number of class I cyt c sequences, and for hh and yeast iso-1-cyt c this lysine is involved in ligand-exchange events occurring at alkaline pH values.[28–30] To test whether lysine coordination plays a role in the unfolding of cyt c-550, all lysine residues were first chemically modified, thereby rendering them incapable of binding to the heme. More specifically, K99 in cyt c-550 is homologous to K79 in the mitochondrial proteins, but no lysine is found at position 84 in cyt c-550 (homologous to K73 in hh cyt c). Therefore, only a single variant, K99E, was used to test whether K99 might act as a nonnative ligand to the heme at neutral pH values.

UV/Vis spectroscopy of ferricyt c-550 and variants at pH 4.5

At pH 4.5 the UV/Vis spectrum of cyt c-550 is indicative of a low-spin heme protein with two strong field axial ligands. Upon titration of increasing amounts of guanidinium hydrochloride (Gdm·HCl), the protein starts to unfold, thereby causing the perturbation of a number of electronic absorption bands in the spectrum and the appearance of new bands. One of these, a band at 623 nm which is characteristic of a high-spin species, grows into the spectrum, a result indicating a change from a low- to high-spin heme. We ascribe this to loss of the M100 axial ligand, which is apparent from the concomitant loss of the 695 nm band that is characteristic of methionine–heme ligation.[18] Figure 2A shows the results for the wt protein and the two variants, with Table 1 listing the corresponding two-state equilibrium unfolding parameters (midpoint concentrations, C_m, slopes, m, and the derived free energy in the absence of denaturant, ΔG_{unf}). For the K99E and H118Q variants the thermodynamic parameters are within the error for the wt protein. This indicates that their respective stabilities, at least under these conditions, are unaltered upon introduction of the point mutations.

Peroxidase activity of ferricyt c-550 and variants at pH 4.5

In the presence of hydrogen peroxide, cyt c-550, like other ferricyts c, is able to catalyze H_2O_2 reduction with concomitant oxidation of a reducing substrate.[31] The rate, however, is ex-

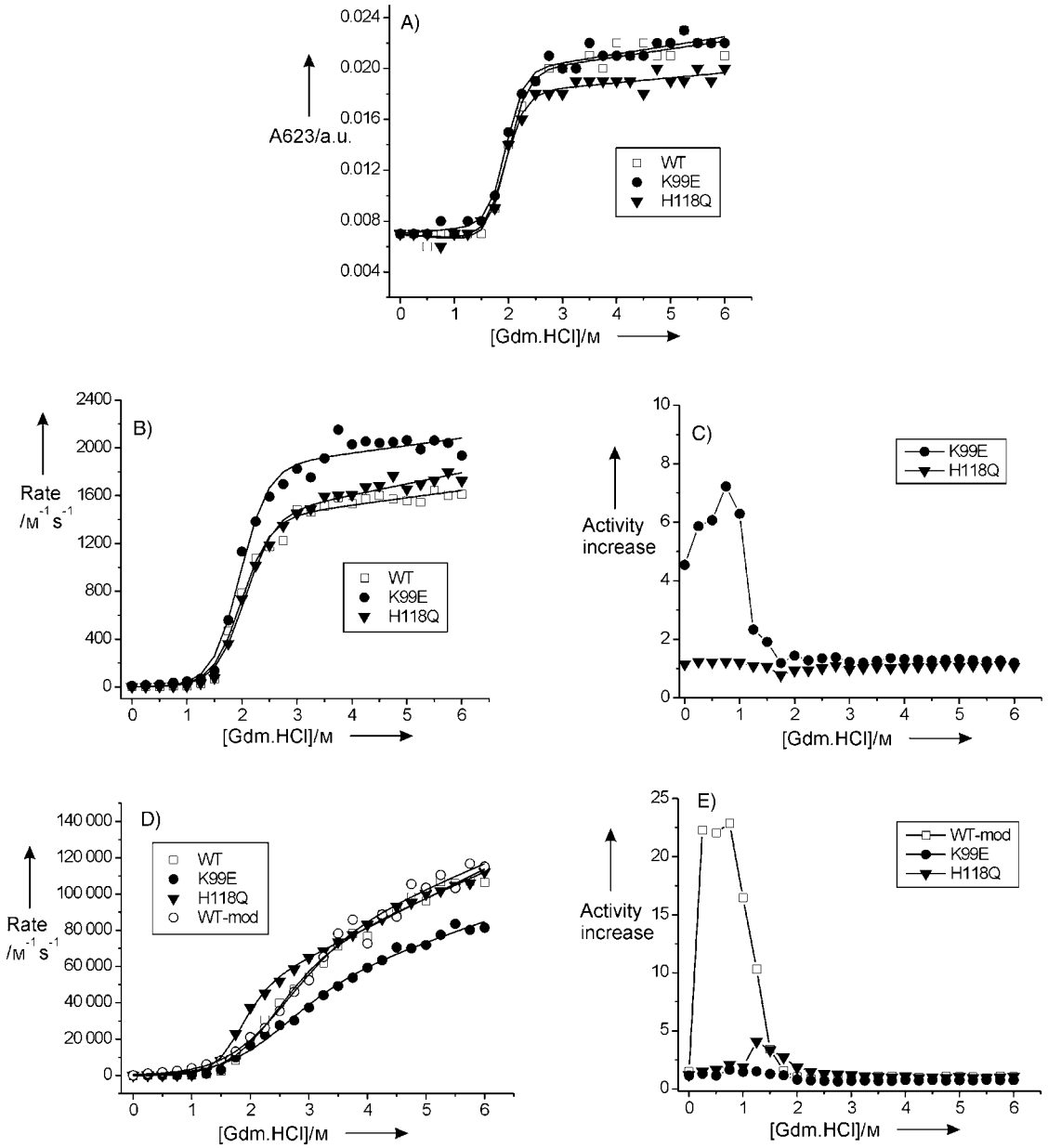

Figure 2. *Equilibrium unfolding at 298 K in the presence of Gdm·HCl for wt ferricyt c-550 and various forms, as monitored by A) the intensity change of the electronic absorption band at 623 nm at pH 4.5, B) the peroxidase activity increase at pH 4.5, C) the peroxidase activity increase as a ratio (variant:wt) of the second-order rate constant at pH 4.5, D) the peroxidase activity increase at pH 7.0, and E) the peroxidase activity increase as a ratio (variant:wt) of the second-order rate constant at pH 7.0. WT-mod denotes the protein after treatment with O-methylisourea.*

Table 1. *Thermodynamic parameters (pH 4.5, 298 K) for the equilibrium unfolding of wt ferricyt c-550 and variants in the presence of Gdm·HCl, as monitored by the intensity change of the electronic absorbance band at 623 nm and the peroxidase activity increase.*

	Absorbance at 623 nm			Peroxidase activity		
Protein	ΔG_{unf} [kcal mol^{-1}]	m [kcal mol^{-1} M^{-1}]	C_m [M]	ΔG_{unf} [kcal mol^{-1}]	m [kcal mol^{-1} M^{-1}]	C_m [M]
wt	6.4 ± 1.6	3.2 ± 0.8	2.0 ± 1.0	4.5 ± 0.5	2.3 ± 0.3	2.0 ± 0.5
K99E	7.1 ± 1.9	3.6 ± 0.9	2.0 ± 1.0	4.5 ± 0.6	2.3 ± 0.3	2.0 ± 0.6
H118Q	6.2 ± 1.5	3.2 ± 0.7	1.9 ± 0.9	4.5 ± 0.4	2.2 ± 0.2	2.0 ± 0.4

tremely low and this can be assigned to two factors. Firstly, it is the deprotonated form of H_2O_2 that reacts with the heme iron. The pK_a value of H_2O_2 free in solution is approximately 12 and, although its apparent value is lowered by about 4 units by binding the heme iron center, only a small fraction of the peroxide anion is available at neutral or acidic pH values. Secondly, access to the heme for the peroxide anion is blocked due to the presence of six ligands on the iron. Upon addition of Gdm·HCl, the activity is significantly increased for the wt protein and the variants (Figure 2B); this coincides with the loss of the axial methionine ligand. This results in a vacant coordi-

nation site at the heme for the peroxide anion to bind. The data for the peroxidase activity assays were fitted to a two-state equilibrium unfolding model and the thermodynamic parameters are presented in Table 1. In all cases the stabilities, as measured by peroxidase activity increase, are lower than those obtained from the 623 nm measurements.

If it is assumed that unfolding is strictly two-state, then at zero [Gdm·HCl] the fraction of fully unfolded wt protein is 2.49×10^{-5} based on the ΔG_{unf} value obtained from the equilibrium unfolding measurements as monitored at 623 nm. This would correspond to an expected 40000 times increase in peroxidase activity at 6 M Gdm·HCl; yet, from the ratio of activities between native and "fully" unfolded protein, an activity increase of only 770 times is observed. Therefore, at zero [Gdm·HCl], approximately 1.3‰ of the protein is in a form that is peroxidase active but is not the fully unfolded species. Thus, the unfolding curve measured by peroxidase activity is more representative of the transition to the lowest free energy species, as indicated from the lower thermodynamic parameters compared to those measured with UV/Vis spectroscopy (Table 1) and fluorescence spectroscopy.[26,27] Similar observations are observed for the peroxidase activity assays with hh cyt c,[26] where the ΔG_{unf} value obtained from peroxidase activity is comparable to the ΔG_{unf} value for local unfolding of the loop containing the axial methionine at low [Gdm·HCl], as measured by native-state hydrogen-exchange NMR spectroscopy.[2]

In the absence of denaturant the second-order rate constant for the peroxidase activity of the wt protein and the H118Q variant are comparable at pH 4.5 (Table 2), along with their total activity increases upon unfolding. For the K99E variant, however, a fivefold-higher second-order rate constant, relative to that of the wt protein, is found in the absence of Gdm·HCl (Table 2). On comparing the activity ratios (variant:wt) in Figure 2C, it is clear that removal of K99 results in an increased population of a peroxidase-active species between 0–1 M Gdm·HCl. However, at higher Gdm·HCl concentrations the rate is independent of the mutations introduced into the protein, a result suggesting that protein-based ligand-exchange events at pH 4.5, which may affect the peroxidase activity at low [Gdm·HCl], are not occurring at high [Gdm·HCl]. At acidic pH values it is well documented from studies with the mitochondrial proteins that ligand exchange does not occur;[1,5,6] yet removal of K99 in cyt c-550 clearly has an effect on the peroxidase-active form at low denaturant concentrations.

Table 2. *Second-order rate constants, k (298 K), for the reaction of H_2O_2 with various forms of cyt c-550 in the absence of Gdm·HCl, along with the total activity increase (defined as the ratio between the second-order rate constant at 6 M Gdm·HCl and 0 M Gdm·HCl) at the two different pH values.*

	pH 4.5		pH 7.0	
Protein	k [$M^{-1}s^{-1}$]	total increase	k [$M^{-1}s^{-1}$]	total increase
wt	2.1 ± 0.2	770	22.8 ± 0.4	4700
K99E	9.6 ± 0.3	200	26.4 ± 0.4	3100
H118Q	2.6 ± 0.2	720	27.9 ± 0.3	4100
wt-mod[a]	–	–	34.5 ± 0.4	3340

[a] wt-mod denotes the protein after treatment with *O*-methylisourea.

A possible explanation for the above observations can be inferred from the crystal structure of the wt protein (J.A.R.W., unpublished results). Electron density for many of the lysine side chains is absent, most probably due to their high mobility. However, electron density is observed for the side-chain amino group of K99 due to a stabilizing hydrogen-bond interaction with the main-chain carbonyl oxygen atom of K54. Such an interaction results in the side chain of K99 nestling onto the side of the heme, thereby helping to protect the heme cavity from solvent. The loss of a hydrogen-bonding interaction upon replacement with a glutamate residue and the subsequent introduction of a negative charge, along with the probable increased exposure of the heme cavity to solvent, would appear to destabilize either the methionine loop, the metal–ligand interaction, or both; this results in an increased population of a partially unfolded peroxidase-active protein under native and low [Gdm·HCl] conditions. Such a subtle destabilization goes unnoticed in terms of the thermodynamic parameters, but is clearly detected from the peroxidase activity assays.

1D ^{1}H NMR spectroscopy of ferricyt c-550 at pH 4.5

Due to the paramagnetic properties of low-spin ferricyt c-550 ($S=^1/_2$), a number of well-resolved resonances belonging to protons of heme substituents and axial ligands are observed outside of the diamagnetic envelope in the ^{1}H NMR spectrum (Figure 3A). The pattern of heme–methyl signals and the presence of the signal arising from the M100 side-chain methyl protons are indicative of methionine–histidine heme ligation. Between 0 and 1 M Gdm·HCl, the intensity of the native protein signals in the diamagnetic and paramagnetic regions of the spectrum decreases. Further increases in [Gdm·HCl] result in a total loss of the native paramagnetic signals. At 1.5 M Gdm·HCl, peaks appear at a higher frequency in the ^{1}H NMR spectrum, which are not present in the absence of denaturant (Figure 3B). The chemical shifts and line widths are indicative of protons of heme substituents arising from a high-spin ferric heme form. This observation is in accordance with the 623 nm measurements.

The presence of both high- and low-spin heme peaks at 1.5 and 2.1 M Gdm·HCl is indicative of a slow-exchange process on the NMR timescale between at least two species. In principle, the high-spin species could be either a penta-coordinate or hexa-coordinate heme with a water molecule as the sixth ligand; the latter has been shown to exist on the unfolding pathway of hh cyt c from time-resolved resonance Raman spectroscopy.[6] Between 1.5 and 2.1 M Gdm·HCl, the high-spin heme peaks become better resolved with a new peak forming at $\delta=76$ ppm (Figure 3B), whilst at higher denaturant concentrations a general broadening of the new resonances is observed. These observations point towards the presence of a number of different high-spin forms which are exchanging with one another as the protein unfolds. Attempts with

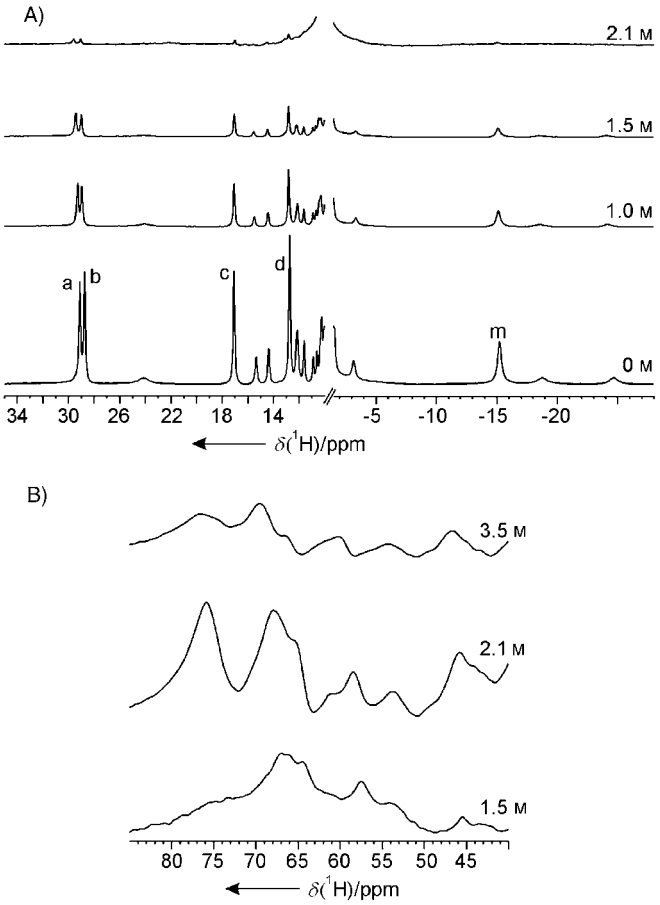

Figure 3. *^{1}H NMR spectra (600 MHz, 298 K) of wt ferricyt c-550 (100 mM NaPi, pH 4.5) in the presence of increasing amounts of Gdm·HCl. In (A) the signals arising from the four hyperfine-shifted heme methyl substituents, 8, 3, 5, and 1, are labeled as a, b, c, and d, respectively, and m corresponds to the side-chain methyl protons of the coordinating M100 ligand. The spectrum at 2.1 M Gdm·HCl has been magnified ten times. In (B) the region of the ^{1}H NMR spectrum containing the new peaks coinciding with increasing [Gdm·HCl] is depicted.*

exchange spectroscopy (EXSY) to assign these high-spin heme peaks proved unsuccessful.

2D NMR spectroscopy of ^{15}N-labeled wt ferricyt c-550 at pH 4.5

Further insight into the unfolding by analysis of the polypeptide chain in the presence of Gdm·HCl was obtained by ^{1}H–^{15}N HSQC experiments at pH 4.5. Chemical shift variations for the native amide peaks were observed at all Gdm·HCl concentrations for which they were still visible (0.5–1.5 M Gdm·HCl). These shifts most likely arise from a combination of increasing ionic strength and the binding of Gdm·HCl to the protein surface. Recent work has highlighted the fact that Gdm·HCl has no recognizable hydration shell and is therefore not retained in the bulk solvent but preferentially binds to the protein surface.[32] In Figure 4, the average amide chemical shift changes upon increasing [Gdm·HCl] are plotted against residue number. It is apparent that the binding of Gdm·HCl to the protein is highly aspecific with many regions of the structure affected. The largest chemical shift changes ($\Delta\delta \geq 0.2$ ppm) occur in parts of the structure away from the N- and C-terminal helices and involve residues 47–49, 56–57, 73, 84, 88, 98, 101, 102, and 105. It is interesting to note that the regions 47–49, 56–57, and 101–102 are involved in hydrogen-bonding interactions with buried water molecules in the heme cavity, a fact suggesting that Gdm·HCl may disrupt these interactions.

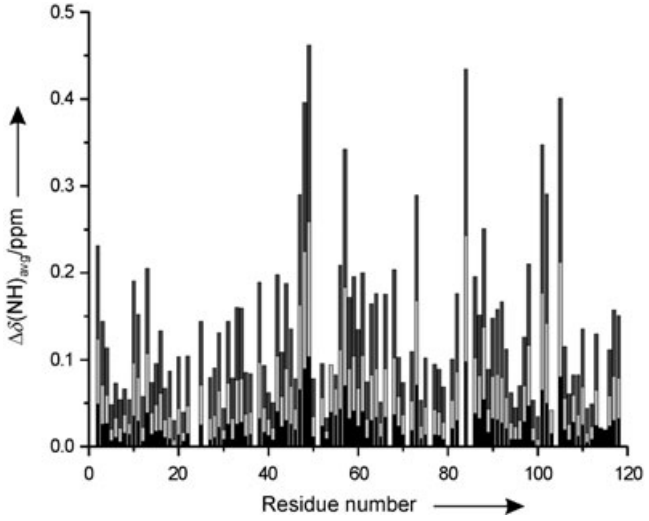

Figure 4. *Average amide chemical shift changes versus residue number for wt ferricyt c-550 at pH 4.5 and 298 K in the presence of 0.5 M (black), 1.0 M (light gray), and 1.5 M (dark gray) Gdm·HCl.*

In addition to the native amide signals, new peaks appear in the spectrum at 1.5 M Gdm·HCl (Figure S1 in the Supporting Information). The observation of a new polypeptide form at the same time as the native fold is consistent with the 1D NMR experiments, where two species differing in heme ligation state are in slow exchange with one another on the NMR timescale. With an increase in [Gdm·HCl] or temperature, the native peaks further decrease in intensity and the new amide peaks predominate (Figure S1 in the Supporting Information). The small chemical shift dispersion in the ^{1}H dimension (approximately 1 ppm) relative to that of the native peaks is indicative of a polypeptide lacking tertiary and secondary interactions.

^{15}N relaxation of wt ferricyt c-550 in the absence and presence of Gdm·HCl at pH 4.5

^{15}N relaxation can be used to obtain an insight into the dynamics of the polypeptide chain on the nano- to picosecond timescale.[33] The ^{15}N relaxation times, T_1 and T_2, and the $\{^{1}H\}^{15}N$ nOe value have been measured for all nonoverlapping amide cross-peaks in the ^{1}H,^{15}N HSQC spectrum for the folded protein in the absence and presence of Gdm·HCl. The relaxation parameters are plotted in Figure 5, and the 10% trimmed mean values and errors are given in Table 3.[34] From the T_1/T_2 ratio in the absence of denaturant, a correlation time (τ_r) for the overall tumbling of the molecule in solution of 6.5 ± 0.2 ns is calculated.[34] This value is in line with other proteins of similar shape and size and is in good agreement with the τ_r value determined for ferrocyt c-550 (6.6 ns).[35] Some residues display

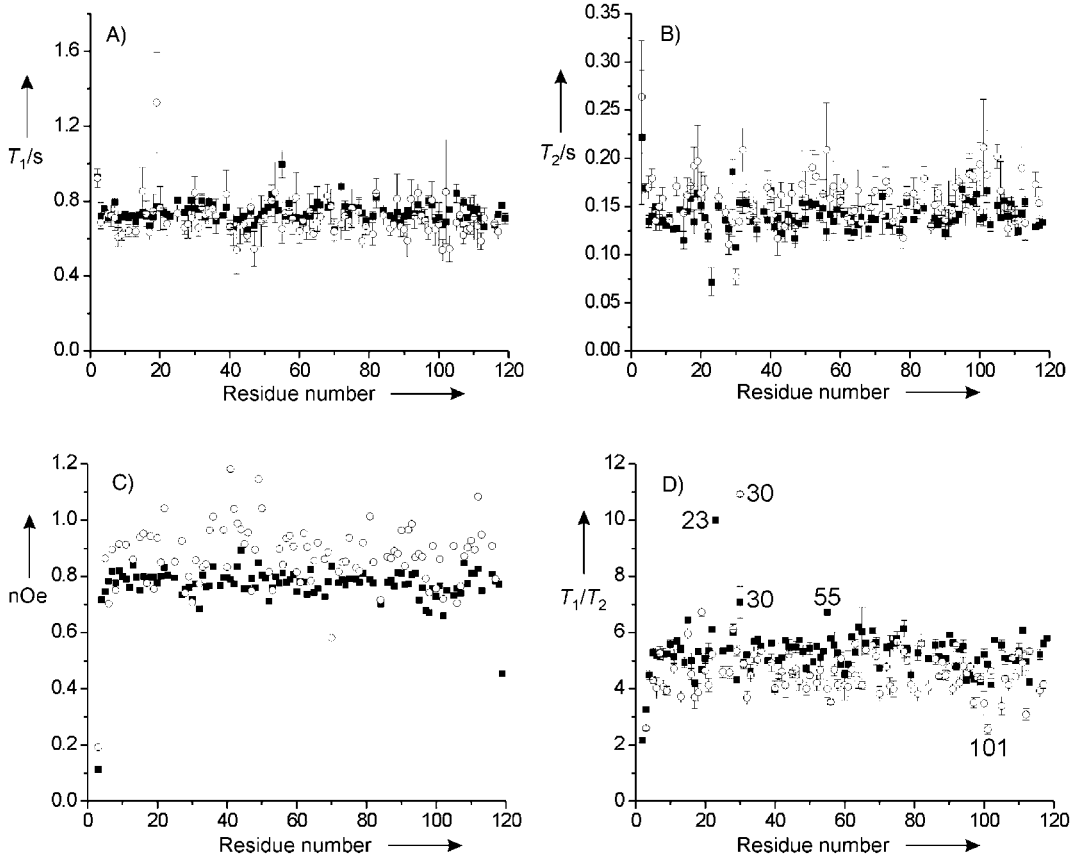

Figure 5. ^{15}N relaxation data and {^{1}H}^{15}N nOe values for wt ferricyt c-550 (20 mM sodium acetate, pH 4.5, 100 mM NaCl) in the absence (■) and presence of 1.5 M Gdm·HCl (○) at 298 K. The numbers on the T_1/T_2 plot indicate residues that have a ratio above or below the mean, as discussed in the text.

Table 3. *10% trimmed average T_1 and T_2 values (seconds), ^{15}N nOe values, and T_1/T_2 ratios for backbone amide ^{15}N nuclei of folded wt cyt c-550 in the absence and presence of Gdm·HCl and the average values for nonnative amide peaks in the presence of Gdm·HCl (14.1 T, 20 mM sodium acetate, pH 4.5, 100 mM NaCl, 298 K).*

	Folded protein zero denaturant	Folded protein 1.5 M Gdm·HCl	Unfolded protein 1.5 M Gdm·HCl
T_1	0.74 ± 0.02	0.70 ± 0.06	1.83 ± 0.2
T_2	0.14 ± 0.01	0.16 ± 0.02	0.67 ± 0.1
nOe	0.78	0.88	−0.45
T_1/T_2	5.4 ± 0.2	4.6 ± 0.2	2.7 ± 0.7

values that are more than one standard deviation below or above the mean ratio. The latter are indicative of a contribution of slow (micro- to millisecond timescale) conformational exchange to the T_2 value[36] and include residues A23, V30, and Y55. A23 and V30 are situated in a loop region on the axial histidine side of the heme protruding out into the solvent (Figure 1), whereas Y55 is located on a loop protecting the side of the heme with its side-chain phenolic oxygen atom forming a hydrogen bond with one of the heme propionate groups. Residues with mean T_1/T_2 values slightly below the average occur predominately in the loop region harboring the M100 axial ligand and include A95, A96, K97, K99, and F102 (Figure 1). In the {^{1}H}^{15}N nOe measurements, the same residues have slightly decreased nOe values compared to the average and this is indicative of fast internal motions.[36] Also noteworthy are the low nOe values at the N terminus for E2 (negative nOe, not shown) and G3 and also for S119 after the C-terminal helix; these values suggest increased flexibility. Furthermore, a number of unassigned amide peaks display negative nOe values. These peaks, in analogy with the assignment data on the ferrous form,[35] arise from a 13 residue amino acid extension preceeding the C-terminal helix; from the negative nOe values, this extension is deemed highly mobile and unstructured in both oxidation states of the protein.

In general, the rather uniform relaxation parameters indicate that the main chain of ferricyt c-550 is fairly rigid on the nano- to picosecond timescale. Such a conclusion was also inferred from a ^{15}N mobility study with the ferrous form,[35] with the same backbone regions indicating slight deviations from the mean relaxation values as were observed here. Other ^{15}N mobility studies with bacterial cyts c in the ferric state have also revealed little variation in relaxation parameters, a fact suggesting highly rigid structures.[37–39] The only other ^{15}N mobility study in which both redox states of a bacterial cyt c have been analyzed is the cyt c-553 from the Gram-positive bacterium *Bacillus pasteurii*.[37,40] This class I cytochrome consists of only 71 amino acids with little variation in mobility on the nano- to picosecond timescale between the two redox states reported. Cyt c-550 is almost twice the size of the "minimal" cyt c-553;

yet despite the additional amino acid inserts, global rigidity on the nano-to picosecond timescale is retained in both oxidation states. In contrast, mitochondrial yeast iso-1-cyt c displays more pronounced mobility differences between the two redox states.[41–43] The ferric form shows higher global flexibility, especially in the loop region containing the axial methionine ligand,[42,43] with several residues belonging to helical segments in yeast iso-1-cyt *c* exhibiting conformational exchange on the micro- to millisecond timescale.[41]

From peroxidase activity assays at pH 4.5 with the mitochondrial hh and yeast iso-1-cyts c, the ΔG_{unf} value assigned to local unfolding of the axial methionine loop was found to be lower than with the bacterial proteins, *Pseudomonas aeruginosa* cyt c-551 and *Paracoccus versutus* cyt c-550.[26] If it is assumed that the methionine–Fe^{III} bond strength is invariant between the different species, then other factors contributing to the enhanced stability of the bacterial proteins towards denaturant must be considered. One such consideration on comparing the available dynamics data for bacterial cyts c with their mitochondrial counterparts is the extent of plasticity in the axial ligand loop. The apparent stiffening of this region in the bacterial proteins seemingly plays a role in determining the equilibrium of the dynamic exchange process causing release of the axial methionine ligand.[44]

As the HSQC spectrum in the presence of Gdm·HCl has the same fingerprint as the folded form, albeit with chemical shift changes, this species can still be considered as a native form. The presence of Gdm·HCl, up to 1.5 M, appears to have little effect on this form in terms of the relaxation properties (Table 3 and Figure 5). A marginal decrease in the mean T_1/T_2 ratio translates to a lower τ_r value of 5.7 ± 0.6 ns. V30 displays an increased T_1/T_2 ratio in the absence of Gdm·HCl, a fact relating to an increased conformational exchange process that possibly involves an unfolded form of the protein (Figure 5). The resonance arising from A23, which exhibits a high T_1/T_2 ratio in the absence of Gdm·HCl (Figure 5), is not observed at 1.5 M Gdm·HCl due to peak overlap, while T101 displays a mean T_1/T_2 value below the average, a fact suggesting increased internal motions in this region.[36] No new extensive conformational exchange processes were observed, in contrast to a previous report with *B. pasteruii* cyt c-553 in the presence of Gdm·HCl.[20] The most visible change is for the $\{^1H\}^{15}N$ nOe measurement, where an erratic variation in nOe values is observed (Figure 5), with the mean value increasing to 0.88 in the presence of 1.5 M Gdm·HCl. Such an increase would suggest a stiffening of the structure with highly restricted internal motions. This is unlikely, however, as the effect of the denaturant would be expected to loosen the structure. An explanation for the observed effect at elevated [Gdm·HCl] on the nOe values is therefore unclear.

As mentioned, at 1.5 M Gdm·HCl, new peaks are observed in the HSQC spectrum, which from the poor chemical shift dispersion in the ^1H dimension are assigned to an unfolded form. For a number of these new nonnative peaks (25 nonoverlapping cross-peaks) it was possible to extract relaxation parameters, with the average values presented in Table 3. The large increases in both T_1 and T_2 times and the negative nOe values further confirm an unfolded species lacking in tertiary and secondary interactions. These findings differ from the unfolding of yeast iso-1-cyt c in the presence of sodium dodecylsulfate, where the dynamics data for the nonnative resonances in the $^1H,^{15}N$-HSQC spectrum indicate a compact structure with residual helical content.[45]

Peroxidase activity of wt and lysine-modified ferricyt c-550 at pH 7.0

The unfolding transition at pH 7.0 monitored by peroxidase activity increase for the wt protein and the variants is shown in Figure 2D, and the thermodynamic parameters obtained from the fitting are given in Table 4. In nearly all cases, with the possible exception of the H118Q variant, the relative steepness of the posttransitional baseline complicates the fitting procedure, causes a shift in the transitional midpoint and affects the outcome of the thermodynamic parameters. Such a sloping baseline has been explained as being due to an increase in protein volume, which lowers the effective concentration of protein-based heme ligands that inhibit the activity.[26] However, when peroxidase activity in urea (data not shown) is monitored no such increase in posttransitional baseline is observed, a result suggesting that the type of denaturant also has an effect (ionic versus neutral). The second-order rate constant for the reaction with H_2O_2 and the total activity increase for the wt protein upon unfolding under nondenaturing conditions are given in Table 2. The higher total activity increase compared to that at pH 4.5 may, in part, be related to there being less of the lowest energy intermediate present under native conditions due to a more stable methionine–iron interaction at pH 7.0.

Table 4. *Thermodynamic parameters (pH 7.0, 298 K) for the equilibrium unfolding of various forms of ferricyt c-550 in the presence of Gdm·HCl, as monitored by the peroxidase activity increase.*

Protein	ΔG_{unf} [kcal mol^{-1}]	m [kcal mol^{-1} M^{-1}]	C_m [M]
wt	3.2 ± 0.4	1.4 ± 0.2	2.3 ± 0.6
K99E	2.5 ± 0.2	1.1 ± 0.1	2.4 ± 0.4
H118Q	4.5 ± 0.5	2.5 ± 0.3	1.8 ± 0.3
wt-mod	2.6 ± 0.3	1.1 ± 0.2	2.4 ± 0.7

Upon treatment of the wt protein with *O*-methylisourea, lysine residues are converted into homoarginine, thereby rendering them incapable of acting as ligands to the heme. On comparing the activity ratio (lysine-modified:wt; Figure 2E), it is apparent that the lysine modification has an effect on peroxidase activity at low [Gdm·HCl]. A 22 times higher activity of lysine-modified protein versus the wt protein is observed between 0 and 1 M Gdm·HCl. This increase in the peroxidase-active form can be correlated to the removal of a ligand(s), which in a partially unfolded form inhibits the activity. Alternatively, it may be interpreted that the modification results in a less stable protein. However, in terms of local unfolding, the

C_m value measured by peroxidase activity is, within error, the same as that of the wt protein (Table 4).

1D ^{1}H NMR spectroscopy of wt ferricyt c-550 at pH 7.0

At pH 7.0, signals arising from the heme substituents and the axial methionine ligand decrease in intensity as [Gdm·HCl] is increased (Figure 6). Furthermore, the native 8 and 3 heme

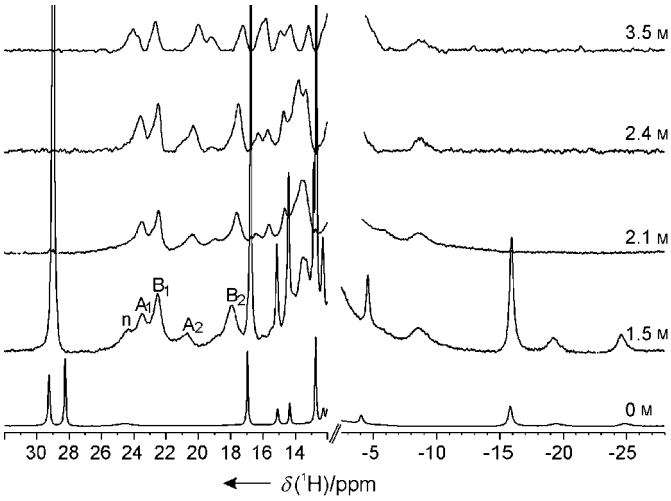

Figure 6. *^{1}H NMR spectra (600 MHz, 298 K) of wt ferricyt c-550 (100 mM NaPi, pH 7.0) in the presence of increasing amounts of Gdm·HCl. The signals labeled A_1, A_2, B_1, and B_2 arise from nonnative heme ligation and n corresponds to a native peak of the protein. The spectra are not of equal intensity.*

methyl proton peaks ($\delta = 29.2$ and 28.3 ppm) shift up- and down-field, respectively, thereby resulting in the formation of a single peak. Such an observation has previously been reported for cyt c-550 as a function of increasing ionic strength at neutral pH values.[46] At 1.5 M Gdm·HCl, a number of new broader peaks are observed in the spectrum (Figure 6). The observation of peaks arising from both native and nonnative forms of the protein is again consistent with a slow-exchange regime on the NMR timescale. The positions in the spectrum of the nonnative peaks at $\delta = 12$–25 and -8.6 ppm, give a strong indication that they are hyperfine-shifted protons of heme substituents arising from a new low-spin form(s) of the protein. Conceivably, the peak at $\delta = -8.6$ ppm could also arise from protons of the native H19 ligand.[47] These observations confirm that ligand exchange is occurring. Unlike the spectrum at pH 4.5, no peaks at higher frequency corresponding to a high-spin heme form were observed. At elevated [Gdm·HCl], the nonnative signals start to decrease in intensity, as evidenced by the signal-to-noise ratio, but remain visible above 3.5 M Gdm·HCl, when the protein is considered to be in an unfolded state.

Identification of the nonnative ligands on the heme by T_1 relaxation measurements at pH 7.0

Proton signals arising from heme methyl groups are extremely sensitive to the type of axial ligands on the heme.[48] If the methionine ligand is replaced with either an exogenous or protein-based ligand, a change occurs in the distribution of the unpaired electron spin density on the heme, which becomes manifest in a change in the T_1 relaxation times for protons of the heme methyl peaks.[49] T_1 relaxation times for the native heme methyl peaks in the absence and presence of Gdm·HCl are given in Table 5 and are indicative of methionine–histidine

Table 5. *T_1 times [ms] for heme methyl protons of various forms of ferricyt c-550 with native and nonnative heme ligation at pH 7.0.*

Protein	Histidine/ methionine	Histidine/ lysine	A_1+A_2	B_1+B_2
wt	95–100			
M100K		150–180		
wt(Gdm·HCl)	90–100		120–150	53–57
wt-mod(Gdm·HCl)	85–95			51–53
H118Q(Gdm·HCl)	100–105		142	

heme ligation. Although the nonnative peaks at $\delta = 23.5$, 22.5, 20.7, and 17.9 ppm are broader and more crowded than the native heme methyl signals, the T_1 times could be measured (Figure S2 in the Supporting Information). The peaks at $\delta =$ 23.5 and 20.7 ppm (A_1 and A_2 in Figure 6) have significantly longer T_1 times than the peaks at $\delta = 22.5$ and 17.9 ppm and also the native peaks (Table 5). This suggests that they arise from heme methyl groups in which a deprotonated side-chain amino group of a lysine residue(s) or the α-amino group of the N terminus is coordinating to the heme.[8,50] The latter possibility can be ruled out, as in cyt c-550 the N-terminal glutamine residue is pyroglutamated. Although the pK_a value of a lysine is approximately 10.8, evidence exists from studies on the alkaline transition of cyts c that the events prior to release of the methionine ligand and the subsequent formation of the strong lysine–iron bond can significantly lower the apparent pK_a value of a lysine.[51,52] Longer T_1 times for heme methyl groups of a cytochrome with lysine–histidine heme coordination were confirmed from measuring the relaxation times of the M100K variant, where the axial M100 ligand is replaced with a coordinating lysine residue (Table 5).[53] The peaks at $\delta = 22.5$ and 17.9 ppm (B_1 and B_2 in Figure 6) gave much shorter T_1 times than the native peaks and are in the range for histidine–histidine coordination (Table 5).[8,9] These results point towards the presence of three species at 1.5 M Gdm·HCl: the native form and two nonnative low-spin heme forms. A fourth high-spin form is also inferred from the peroxidase activity assays, but due to its low population is not observed by NMR spectroscopy.

Additional support for the nonnative ligand type on the heme comes from the ^{1}H NMR spectrum of the lysine-modified protein, in which peaks A_1 and A_2 assigned with lysine coordination have disappeared and peaks B_1 and B_2 assigned with histidine coordination remain (Figure 7). Upon addition of KCN (final concentration 3 mM) to the lysine-modified protein in the presence of Gdm·HCl, peaks B_1 and B_2 decrease dramatically in intensity and heme methyl signals of a CN^--bound form

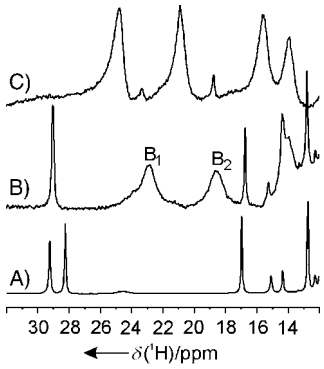

Figure 7. *^{1}H NMR spectra (600 MHz, pH 7.0, 298 K) of lysine-modified ferricyt c-550 A) in the absence of Gdm·HCl, B) in 1.5 M Gdm·HCl, and C) after the addition of 3 mM KCN to (B). Peaks labeled B_1 and B_2 have similar chemical shifts and T_1 relaxation times to the analogous signals observed for the wt protein.*

predominate (Figure 7).[54] It is noted that peaks B_1 and B_2 are still present but are of much lower intensity and appear to be sharper (Figure 7). The latter may indicate that the histidine–histidine form giving rise to the broad signals assigned as B_1 and B_2 is in exchange with multiple unfolded species, whereas this is no longer the case in the presence of CN^-. Two peaks ($\delta = 25.0$ and 21.0 ppm) of the CN^--bound form have very similar chemical shifts to the A_1 ($\delta = 23.5$ ppm) and A_2 ($\delta =$ 20.7 ppm) signals, which were assigned with lysine–heme coordination. As CN^- and lysine coordination have a similar effect on the electronic structure of the heme in terms of heme methyl chemical shifts,[54] this provides further evidence that A_1 and A_2 arise from lysine coordination.

In comparison with hh cyt c, the same nonnative protein ligands on the heme (lysine and histidine) are observed upon release of the methionine ligand.[7,8] Subtle differences are, however, apparent. For hh cyt c, heme methyl signals assigned to two lysine conformers (akin to the alkaline transition[29]) are observed at low denaturant concentrations and are replaced at higher denaturant concentrations with heme methyl signals assigned to two histidine–histidine species (H26 and H33).[8] For cyt c-550, no gradual replacement of one set of nonnative signals by another occurs. Instead, new signals appear in a concerted manner and are still detectable, albeit less intense, at Gdm·HCl concentrations greater than 3.5 M. Furthermore, no evidence for two lysine conformers is observed. This is also the case for the alkaline transition in cyt c-550, where a single coordinating lysine species is observed by NMR spectroscopy.[55]

The effect of the K99E mutation on unfolding at pH 7.0

The second-order rate constant for the peroxidase activity and the total activity increase for the K99E variant at pH 7.0 are given in Table 2. The unfolding curve is shown in Figure 2D and thermodynamic parameters obtained from the fitting are given in Table 4. From the activity ratio in Figure 2E little increased activity relative to the wt protein is observed at any [Gdm·HCl]. Thus, unlike the situation at pH 4.5, no increased activity is observed at low denaturant concentrations. Furthermore, it suggests that, at pH 7.0, K99 is not a ligand to the heme as the protein unfolds. This is also concluded from the ^{1}H NMR spectrum in the presence of Gdm·HCl, with the peaks A_1 and A_2 that were assigned with lysine coordination in the wt protein still present in the K99E spectrum (Figure S3 in the Supporting Information).

The effect of the H118Q mutation on unfolding at pH 7.0

In the absence of denaturant at pH 7.0, the second-order rate constant for the peroxidase activity and the total activity increase for the H118Q mutation are comparable to that for the wt protein (Table 2), but the unfolding curve generated from the peroxidase activity assay (Figure 2D) is more cooperative (see also the thermodynamic parameters in Table 4). A significantly increased activity relative to that of the wt protein is observed between 1.25 and 2 M Gdm·HCl, a fact suggesting that H118 acts as a heme ligand in a fraction of partially unfolded wt protein and that its absence results in enhanced peroxidase activity. The activity ratio at high [Gdm·HCl] is 1, a result suggesting that H118 misligation is not important in the unfolded state in terms of suppressing the peroxidase activity. However, from the wt protein NMR spectrum at high [Gdm·HCl] (Figure 6), it can be noted that signals arising from a low-spin heme species are present, a result suggesting that a six-coordinate heme form is still populating a significant fraction of the denatured state.

The ^{1}H spectrum of the H118Q variant at pH 7.0 in the presence of Gdm·HCl (Figure 8) has peaks at $\delta = 23.5$ and 20.7 ppm with chemical shifts and T_1 times very similar to the nonnative heme methyl peaks A_1 and A_2 assigned with lysine–heme coordination in the wt protein spectrum (Table 5). The peaks B_1 and B_2 that were assigned to histidine–heme ligation are no longer present, a fact providing evidence that H118 is a non-

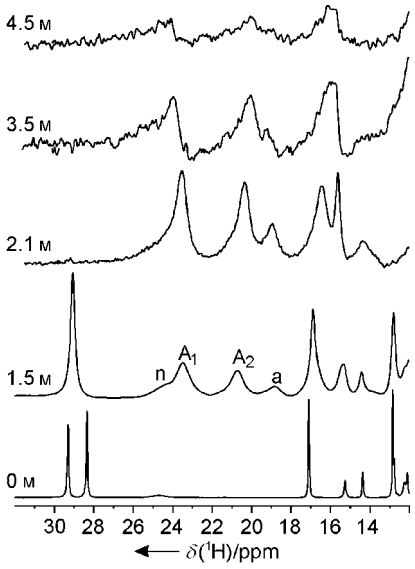

Figure 8. *^{1}H NMR spectra (600 MHz, pH 7.0, 298 K) of the H118Q variant of ferricyt c-550 in the presence of increasing amounts of Gdm·HCl. Peaks labeled A_1 and A_2 have similar chemical shifts and T_1 relaxation times to the analogous signals of the wt protein, as discussed in the text, while n arises from the native form.*

native ligand to the heme in the presence of Gdm·HCl. The peak at $\delta = 18.8$ ppm labeled a in Figure 8 appears earlier in this variant than it does for the wt (Figure 6) and K99E proteins. This peak arises from an unfolded form of the protein and the fact that it appears earlier in the spectrum for the H118Q variant is in line with the unfolding measured from the peroxidase activity (Figure 2D). Also noteworthy is the increased intensity and line broadening of the nonnative peaks relative to the native signals; this suggests an increased population and possible exchange with other unfolded species. At higher denaturant concentrations, the native peaks disappear and a gradual decrease in the intensity of the nonnative form is observed. The signal-to-noise ratio at high [Gdm·HCl] makes it difficult to ascertain whether these nonnative signals are from the same species as those at low [Gdm·HCl], but the results still suggest the presence of a low-spin heme species as expected from the high- to low-spin pK_a values.[27]

All of the bacterial cyts c for which the folding/unfolding has been investigated have lacked a potential nonnative His ligand[21–23] and thereby result in a high-spin heme form in an unfolded state at neutral pH values. Despite this, evidence exists that the cooperative unfolding units correlate well with the mitochondrial proteins.[56] Results from the present study support histidine–heme misligation, but more so at low denaturant concentrations. At higher denaturant concentrations a low-spin species is still present, but it is not clear what this form arises from. Nevertheless, the position of H118 in the sequence of cyt c-550 is distinctly different to the relative positions of the nonnative ligating histidine residues in mitochondrial cyts c, which when ligated to the heme in a denatured state do not interfere with the proposed early folding or late unfolding intermediate with interacting N- and C-terminal helices.[13] For cyt c-550 it is difficult to see how ligation of H118 to the heme would allow the formation of such an intermediate. It may be that this intermediate form does not exist for cyt c-550. This is also inferred from kinetic studies on the folding of *Rhodobacter capsulatus* cyt c_2, a bacterial cytochrome with high structural homology to *Paracoccus versutus* cyt c-550 but lacking a potential nonnative histidine ligand.[23]

Conclusion

In summary, this work shows that peroxidase activity assays and 1D NMR spectroscopy are two complimentary techniques which provide valuable information on the state of the heme as ferricyt c-550 unfolds. Both techniques are most informative under low denaturant concentrations. This is clearly illustrated at pH 7.0 where partially unfolded misligated heme species with lysine and histidine coordination have been identified through 1D NMR spectroscopy, and at low denaturant concentrations, with the aid of protein modifications, such forms are shown to inhibit the peroxidase activity. At higher denaturant concentrations, when the protein is considered to be unfolded, the NMR data are still consistent with the presence of a six-coordinate low-spin heme species. For the mitochondrial proteins it is generally accepted that bis-histidine coordination prevails at neutral pH values in an unfolded state. However, removal of H118 in cyt c-550 still results in a low-spin heme species (Figure 8). Therefore, regardless of which inhibiting ligand is removed, the effect on peroxidase activity at high denaturant concentrations appears to be unaffected.

In hh cyt c, a sequence of ligand-exchange events occurs on going from low to high denaturant concentrations.[7,8] For cyt c-550 this is not the case. The species assigned with lysine–histidine and bis-histidine coordination occur at the same denaturant concentration (1.5 M and above; Figure 6). Involvement of H118 even at low denaturant concentrations suggests that this species must be considerably unfolded. It may be that for cyt c-550 these misligated forms are just two subsets of numerous unfolded species on different pathways, which with increasing denaturant concentrations do not interchange ligands as they become more unfolded.

The mobility study at pH 4.5 adds to the growing body of evidence that bacterial cyts, irrespective of size, have a higher global rigidity than their mitochondrial counterparts. In particular, a stiffening of the axial methionine ligand loop may be one of the reasons why the ΔG_{unf} value inferred from peroxidase activity measurements is higher for bacterial species than for the mitochondrial proteins. The effect on the peroxidase activity of the K99E mutation at pH 4.5 goes some way to illustrating this point.

Finally, the use of cyts c as green catalysts in oxidative chemistry is an attractive alternative to true peroxidases, the latter often being unstable under extreme conditions. For cyts c, harsh conditions are a prerequisite for enhanced activity, and the fact that their peroxidase activity can be regulated by manipulating their conformational state is an advantage. However, as shown in this study, to maximize activity in a nonnative conformational state (partially unfolded form) then elimination of inhibiting protein-based ligands, which suppress activity under nonacidic conditions, must also be considered.

Experimental Section

Construction of *Paracoccus versutus* cyt c-550 variants: The K99E variant of *Paracoccus versutus* cyt c-550 was constructed as previously described.[57] The modification encoding the H118Q mutation was introduced in a single step by site-directed mutagenesis following a procedure based on Stratagene's QuickChange Mutagenesis kit and by using plasmid pMU19 containing the gene for the wt cyt c-550 as the template.[19]

Expression and purification of *Paracoccus versutus* cyt c-550 and variants: Wild-type cyt c-550 was heterologously expressed in *Pseudomonas denitrificans* strain 2131 containing the pEG400.Tv1 plasmid. The K99E and H118Q variants were expressed in *Escherichia coli* by using a dual-plasmid strategy. A pUC19 (Amp^r) vector containing the mutated cyt c-550 gene preceded by its periplasmic translocation sequence was used for protein expression. The second plasmid, pEC86 (Cm^r), contains eight cyt c maturation genes to assist with covalent heme attachment.[58] *E. coli* strain MV1190 containing both plasmids was cultured in Luria–Bertani (LB) medium for 8 h until the optical density at 600 nm (OD_{600}) was approximately 0.8. At this point, the cells were induced with 0.5 mM isopropyl-β-D-thiogalactopyranoside (IPTG) and grown semianerobically for a further 16 h, at which time the cells were

harvested. For growth of ^{15}N-labeled cyt c-550, the wt protein was expressed in *E. coli* with the same strategy as outlined above except that the growth medium consisted of a 70:30 mix of M9 minimal medium containing $^{15}NH_4Cl$ (0.5 g L^{-1}) and ^{15}N-labeled OD2 medium (Silantes). The M9 medium contained trace elements and vitamins as described by Cai et al.[59] Purifications of all proteins including the H118Q variant were performed as previously described.[31]

Preparation of lysine-modified cyt c-550 and mass spectroscopy analysis: Preparation of chemically modified cyt c-550, in which all lysine residues were converted into homoarginines, was carried out with *O*-methylisourea hydrogen sulfate (Aldrich) according to a literature method.[60] The expected increase in molecular weight for 15 lysine residues converted into homoarginine is 631 Da. From electrospray-ionization mass spectrometry, an *m/z* of 15 367 Da was observed (observed *m/z* of unmodified protein: 14 737 Da), thereby confirming complete conversion to homoarginine residues. Furthermore, the *m/z* of the wt protein was consistent with a previous report in which the N-terminal glutamine residue is pyroglutamated.[19]

Unfolding monitored by UV/Vis spectroscopy and peroxidase activity: Gdm·HCl was dissolved to a concentration of 8 M in deionized water (Milli-Q) and filtered before use. Solutions ranging from 0–6 M Gdm·HCl were buffered with 100 mM sodium phosphate and the pH value of each solution was measured separately. Protein samples were oxidized by addition of an excess of $K_3[Fe(CN)_6]$ followed by exchange into water by ultrafiltration methods. Protein concentrations were determined spectrophotometrically from the absorbance at 409 nm ($\varepsilon = 132$ mM^{-1} cm^{-1}),[55] with ferricyt c-550/Gdm·HCl mixtures equilibrated overnight at room temperature prior to unfolding experiments.

UV/Vis spectroscopy was carried out on a Shimadzu UVPC-2101PC spectrophotometer fitted with a thermostat. Protein concentrations of approximately 5 μM were used. Peroxidase activity was assayed by using H_2O_2 and guaiacol (*O*-methoxyphenol, Sigma). The reaction was initiated by mixing a volume of ferricyt c-550/Gdm·HCl with an equal volume of freshly prepared H_2O_2/guaiacol/Gdm·HCl. Production of the fourfold-oxidized product of the peroxidase reaction of cyt c-550, 3,3′-dimethoxy-4,4′-biphenoquinone[61] ($\varepsilon_{470} = 26.6$ mM^{-1} cm^{-1})[62] was followed on the above-mentioned spectrophotometer. The resulting activity profiles were analyzed as previously described, with the reaction rate depending linearly on $[H_2O_2]$.[26,31] For coherent graphical representation, the activities are expressed as the biomolecular rate constant of the H_2O_2/cyt c-550 reaction. All assays were performed at 298 K with [guaiacol] = 10 mM, [cyt c-550] = 0.9–1.6 μM, and $[H_2O_2]$ = 0.1–100 mM.

Unfolding curves were assessed by the two-state model of equilibrium unfolding with the assumption of linear baselines for native and unfolded proteins, according to the method of Santoro and Bolen,[63] as desribed by Equation (1), where *a* and *c* correspond to the baselines values of native and fully unfolded protein at zero denaturant concentration, respectively, and *b* and *d* to their respective dependence on [Gdm·HCl]. ΔG_{unf} is the Gibbs free energy of unfolding in the absence of denaturant and *m* represents the dependence of the unfolding free energy on [Gdm·HCl].

$$\text{observable} = \frac{a+b[\text{Gdm}\cdot\text{HCl}]+(c+d[\text{Gdm}\cdot\text{HCl}])\exp\left(\frac{-\Delta G_{unf}+m[\text{Gdm}\cdot\text{HCl}]}{RT}\right)}{1+\exp\left(\frac{-\Delta G_{unf}+m[\text{Gdm}\cdot\text{HCl}]}{RT}\right)} \quad (1)$$

For the fitting of the peroxidase activity data, the following modification was applied. Since the native state is assumed to be fully inactive due to the six-coordinate heme iron being unable to react with H_2O_2, its activity cannot change linearly with increasing [Gdm·HCl]. Therefore, *a* and *b* (pre- and posttransitional baseline values) in Equation (1) were set to zero. The fits (nonlinear least-squares fitting) were generated by using the algorithm of Levenberg and Marquardt and performed in the program Origin, version 6.0 (Microcal Software, Northampton, MA).

NMR spectroscopy: Samples to be analyzed by NMR spectroscopy contained the desired concentrations of ferricyt c-550 (0.5–1.5 mM), Gdm·HCl (0–4.5 M), 100 mM sodium phosphate or sodium acetate, and 6% D_2O for lock. The pH value of each sample was adjusted to the desired pH value by addition of stock solutions of HCl or NaOH. All experiments were performed on a Bruker DMX600 spectrometer operating at ^1H and ^{15}N frequencies of 600.1 and 60.8 MHz, respectively, and at a temperature of 298 K. 1D ^1H spectra were acquired with presaturation of the residual water signal with a spectral window of 70 ppm. For detection of high-spin heme signals, a 1D WEFT pulse sequence with a delay time of 50 ms and a spectral window of 200 ppm was used. Proton T_1 values were measured by using an inversion recovery pulse sequence with variable delay (VD) times ranging between 0.05–0.9 s. All 1D spectra were processed in XWINNMR, with exponential multiplication (50–200 Hz) being applied to each free induction decay before Fourier transformation. Proton T_1 relaxation times were obtained by fitting the peak intensity as a function of the VD time to a three-parameter single-exponential decay.

Chemical shift perturbations of ^{15}N and ^1H nuclei in the presence of Gdm·HCl were analyzed in the assignment program ANSIG.[64] The average amide chemical shift perturbation ($\Delta\delta_{avg}$) upon addition of Gdm·HCl was calculated from Equation (2), in which $\Delta\delta_N$ represents the change in the chemical shift of the amide nitrogen signal and $\Delta\delta_H$ is the change in chemical shift of the amide proton signal.[65]

$$\Delta\delta_{avg} = \sqrt{\frac{(\Delta\delta_N/5)^2+\Delta\delta_H{}^2}{2}} \quad (2)$$

For ^{15}N longitudinal (T_1) and transverse (T_2) relaxation measurements, 3D versions of ^1H,^{15}N HSQC experiments were implemented by using the pulse sequences described by Kay et al.,[66] in an interleaved fashion with a $^1H(t_2)$–VD–$^{15}N(t_1)$ acquisition order. For both ^{15}N T_1 and T_2 experiments, 256 complex t_1 increments and 2 K t_2 points with 16 scans per t_1 point were employed with spectral widths of 2.1 kHz (^{15}N F_1) and 8.9 kHz (^1H F_3). In the T_1 and T_2 experiments, 10 different VD times ranging from 0.01–1.6 s and 0–0.288 s, respectively, were employed to determine the relaxation times. The relaxation delay between scans was 2.5 s. In both experiments, duplicate points were taken to estimate the experimental error. For the $\{^1H\}^{15}N$ nOe measurements, spectra were collected with and without proton saturation with 320 complex t_1 increments and 2 K t_2 points with 40 scans per t_1 point. An initial delay of 3.5 s was used in the nOe measurements, followed by either a saturation period or a delay of 2.5 s. All spectra were Fourier-transformed in the AZARA program (available from ftp://ftp.bio.cam.ac.uk/pub/azara) and analyzed in the ANSIG program.[64]

Relaxation times were obtained by fitting the peak intensities of the amide resonances as a function of the relaxation delays in the VD lists to a three-parameter single-exponential equation. The standard errors in the fitting parameters were determined from the scatter of the data points around the exponential curve and from

the duplicate relaxation delays in the VD lists. The $\{^1H\}^{15}N$ nOe values were calculated as the ratio of the peak intensity in the spectra with and without saturation.

Acknowledgements

We are grateful for financial support from The Netherlands Organisation for Scientific Research (NWO) under the auspices of the "Softlink" program (grant no.: 98S1010).

Keywords: heme proteins · metalloenzymes · NMR spectroscopy · peroxidases · protein unfolding

[1] M. C. R. Shastry, J. M. Sauder, H. Roder, *Acc. Chem. Res.* **1998**, *31*, 717 – 725.
[2] Y. W. Bai, T. R. Sosnick, L. Mayne, S. W. Englander, *Science* **1995**, *269*, 192 – 197.
[3] S. W. Englander, T. R. Sosnick, L. C. Mayne, M. Shtilerman, P. X. Qi, Y. W. Bai, *Acc. Chem. Res.* **1998**, *31*, 737 – 744.
[4] L. Hoang, S. Bedard, M. M. G. Krishna, Y. Lin, S. W. Englander, *Proc. Natl. Acad. Sci. USA* **2002**, *99*, 12173 – 12178.
[5] S. R. Yeh, S. W. Han, D. L. Rousseau, *Acc. Chem. Res.* **1998**, *31*, 727 – 736.
[6] S. R. Yeh, D. L. Rousseau, *J. Biol. Chem.* **1999**, *274*, 17853 – 17859.
[7] B. S. Russell, R. Melenkivitz, K. L. Bren, *Proc. Natl. Acad. Sci. USA* **2000**, *97*, 8312 – 8317.
[8] B. S. Russell, K. L. Bren, *J. Biol. Inorg. Chem.* **2002**, *7*, 909 – 916.
[9] S. G. Sivakolundu, P. A. Mabrouk, *J. Inorg. Biochem.* **2003**, *94*, 381 – 385.
[10] S. J. Berners-Price, I. Bertini, H. B. Gray, G. A. Spyroulias, P. Turano, *J. Inorg. Biochem.* **2004**, *98*, 814 – 823.
[11] T. Y. Tsong, *J. Biol. Chem.* **1974**, *249*, 1988 – 1990.
[12] S. Oellerich, H. Wackerbarth, P. Hildebrandt, *J. Phys. Chem. B* **2002**, *106*, 6566 – 6580.
[13] G. A. Elove, A. K. Bhuyan, H. Roder, *Biochemistry* **1994**, *33*, 6925 – 6935.
[14] B. Hammack, S. Godbole, B. E. Bowler, *J. Mol. Biol.* **1998**, *275*, 719 – 724.
[15] M. M. Pierce, B. T. Nall, *J. Mol. Biol.* **2000**, *298*, 955 – 969.
[16] S. R. Yeh, S. Takahashi, B. C. Fan, D. L. Rousseau, *Nat. Struct. Biol.* **1997**, *4*, 51 – 56.
[17] S. R. Yeh, D. L. Rousseau, *Nat. Struct. Biol.* **1998**, *5*, 222 – 228.
[18] G. R. Moore, G. W. Pettigrew, *Cytochromes c: Evolutionary, Structural and Physiochemical Aspects*, Springer, Berlin, **1990**.
[19] M. Ubbink, J. Vanbeeumen, G. W. Canters, *J. Bacteriol.* **1992**, *174*, 3707 – 3714.
[20] L. Bartalesi, L. Bertini, K. Ghosh, A. Rosato, P. Turano, *J. Mol. Biol.* **2002**, *321*, 693 – 701.
[21] S. Gianni, C. Travaglini-Allocateli, F. Cutruzzolla, M. Brunori, M. C. R. Shastry, H. Roder, *J. Mol. Biol.* **2003**, *330*, 1145 – 1152.
[22] J. Guidry, P. Wittung-Stafshede, *J. Mol. Biol.* **2000**, *301*, 769 – 773.
[23] J. M. Sauder, N. E. MacKenzie, H. Roder, *Biochemistry* **1996**, *35*, 16852 – 16862.
[24] W. Colon, L. P. Wakem, F. Sherman, H. Roder, *Biochemistry* **1997**, *36*, 12535 – 12541.
[25] J. R. Winkler, *Curr. Opin. Chem. Biol.* **2004**, *8*, 169 – 174.
[26] R. E. M. Diederix, M. Ubbink, G. W. Canters, *Biochemistry* **2002**, *41*, 13067 – 13077.
[27] R. E. M. Diederix, M. Ubbink, G. W. Canters, *ChemBioChem* **2002**, *3*, 110 – 112.
[28] M. Assfalg, I. Bertini, A. Dolfi, P. Turano, A. G. Mauk, F. I. Rosell, H. B. Gray, *J. Am. Chem. Soc.* **2003**, *125*, 2913 – 2922.
[29] X. L. Hong, D. W. Dixon, *FEBS Lett.* **1989**, *246*, 105 – 108.
[30] F. I. Rosell, J. C. Ferrer, A. G. Mauk, *J. Am. Chem. Soc.* **1998**, *120*, 11234 – 11245.
[31] R. E. M. Diederix, M. Ubbink, G. W. Canters, *Eur. J. Biochem.* **2001**, *268*, 4207 – 4216.
[32] P. E. Mason, G. W. Neilson, C. E. Dempsey, A. C. Barnes, J. M. Cruickshank, *Proc. Natl. Acad. Sci. USA* **2003**, *100*, 4557 – 4561.
[33] A. G. Palmer, *Annu. Rev. Biophys. Biomol. Struct.* **2001**, *30*, 129 – 155.
[34] L. E. Kay, D. A. Torchia, A. Bax, *Biochemistry* **1989**, *28*, 8972 – 8979.
[35] M. Ubbink, M. Pfuhl, J. van der Oost, A. Berg, G. W. Canters, *Protein Sci.* **1996**, *5*, 2494 – 2505.
[36] G. M. Clore, P. C. Driscoll, P. T. Wingfield, A. M. Gronenborn, *Biochemistry* **1990**, *29*, 7387 – 7401.
[37] L. Banci, I. Bertini, S. Ciurli, A. Dikiy, J. Dittmer, A. Rosato, G. Sciara, A. R. Thompsett, *ChemBioChem* **2002**, *3*, 299 – 310.
[38] F. Cordier, M. Caffrey, B. Brutscher, M. A. Cusanovich, D. Marion, M. Blackledge, *J. Mol. Biol.* **1998**, *281*, 341 – 361.
[39] B. S. Russell, L. Zhong, M. G. Bigotti, F. Cutruzzola, K. L. Bren, *J. Biol. Inorg. Chem.* **2003**, *8*, 156 – 166.
[40] I. Bartalesi, I. Bertini, A. Rosato, *Biochemistry* **2003**, *42*, 739 – 745.
[41] P. D. Barker, I. Bertini, R. Del Conte, S. J. Ferguson, P. Hajieva, E. Tomlinson, P. Turano, M. S. Viezzoli, *Eur. J. Biochem.* **2001**, *268*, 4468 – 4476.
[42] S. M. Baxter, J. S. Fetrow, *Biochemistry* **1999**, *38*, 4493 – 4503.
[43] J. S. Fetrow, S. M. Baxter, *Biochemistry* **1999**, *38*, 4480 – 4492.
[44] C. Dumortier, J. Fitch, F. Van Petegem, W. Vermulen, T. E. Meyer, J. J. Van Beeumen, M. A. Cusanovich, *Biochemistry* **2004**, *43*, 7717 – 7724.
[45] I. Bertini, P. Turano, P. R. Vasos, A. Bondon, S. Chevance, G. Simonneaux, *J. Mol. Biol.* **2004**, *336*, 489 – 496.
[46] м. Ubbink, G. W. Canters, *Biochemistry* **1993**, *32*, 13893 – 13901.
[47] L. Banci, I. Bertini, G. A. Spyroulias, P. Turano, *Eur. J. Inorg. Chem.* **1998**, 583 – 591.
[48] N. V. Shokhirev, F. A. Walker, *J. Biol. Inorg. Chem.* **1998**, *3*, 581 – 594.
[49] L. Banci, I. Bertini, K. L. Bren, H. B. Gray, P. Turano, *Chem. Biol.* **1995**, *2*, 377 – 383.
[50] S. G. Sivakolundu, P. A. Mabrouk, *Protein Sci.* **2001**, *10*, 2291 – 2300.
[51] L. L. Pearce, A. L. Gartner, M. Smith, A. G. Mauk, *Biochemistry* **1989**, *28*, 3152 – 3156.
[52] M. T. Wilson, C. Greenwood in *Cytochrome c: A Multidisciplinary Approach* (Eds.: R. A. Scott, A. G. Mauk), University Science Books, Sausalito, CA, **1995**, pp. 611 – 634.
[53] M. Ubbink, A. P. Campos, M. Teixeira, N. I. Hunt, H. A. O. Hill, G. W. Canters, *Biochemistry* **1994**, *33*, 10051 – 10059.
[54] R. O. Louro, E. C. de Waal, M. Ubbink, D. L. Turner, *FEBS Lett.* **2002**, *510*, 185 – 188.
[55] A. Lommen, A. Ratsma, N. Bijlsma, G. W. Canters, J. E. Vanwielink, J. Frank, J. Vanbeeumen, *Eur. J. Biochem.* **1990**, *192*, 653 – 661.
[56] I. Bartalesi, A. Rosato, W. Zhang, *Biochemistry* **2003**, *42*, 10923 – 10930.
[57] M. Ubbink, G. C. M. Warmerdam, A. P. Campos, M. Teixeira, G. W. Canters, *FEBS Lett.* **1994**, *351*, 100 – 104.
[58] E. Arslan, H. Schulz, R. Zufferey, P. Kunzler, L. Thony-Meyer, *Biochem. Biophys. Res. Commun.* **1998**, *251*, 744 – 747.
[59] M. L. Cai, Y. Huang, K. Sakaguchi, G. M. Clore, A. M. Gronenborn, R. Craigie, *J. Biomol. NMR* **1998**, *11*, 97 – 102.
[60] T. P. Hettinge, H. A. Harbury, *Biochemistry* **1965**, *4*, 2585.
[61] D. R. Doerge, R. L. Divi, M. I. Churchwell, *Anal. Biochem.* **1997**, *250*, 10 – 17.
[62] D. A. Baldwin, H. M. Marques, J. M. Pratt, *J. Inorg. Biochem.* **1987**, *30*, 203 – 217.
[63] M. M. Santoro, D. W. Bolen, *Biochemistry* **1992**, *31*, 4901 – 4907.
[64] P. J. Kraulis, *J. Magn. Reson.* **1989**, *84*, 627 – 633.
[65] D. S. Garrett, Y. J. Seok, A. Peterkofsky, G. M. Clore, A. M. Gronenborn, *Biochemistry* **1997**, *36*, 4393 – 4398.
[66] L. E. Kay, L. K. Nicholson, F. Delaglio, A. Bax, D. A. Torchia, *J. Magn. Reson.* **1992**, *97*, 359 – 375.
[67] G. W. Bushnell, G. V. Louie, G. D. Brayer, *J. Mol. Biol.* **1990**, *214*, 585 – 595.

Received: August 13, 2004
Published online on March 2, 2005

